<Supporting Information>

Lithium-desorption mechanism in $LiMn_2O_4$, $Li_{1.33}Mn_{1.67}O_4$, and $Li_{1.6}Mn_{1.6}O_4$ according to precisely controlled acid treatment and density functional theory calculations

Aolei Gao,[ab] Xinjuan Hou,*[ab] Zhenhua Sun,[a] Shaopeng Li,*[a] Huiquan Li,*[ab] and Jianbo Zhang [a]

[a] CAS Key Laboratory of Green Process and Engineering, National Engineering Laboratory for Hydrometallurgical Cleaner Production Technology, Institute of Process Engineering, Chinese Academy of Sciences, Beijing 100090, China

[b] University of Chinese Academy of Sciences, Beijing 100049, China

E-mails of corresponding authors: hqli@ipe.ac.cn; xjhou@ipe.ac.cn; shpli@ipe.ac.cn.

Study on exchange energies of $Li_{1.33}Mn_{1.67}O_4$ and $Li_{1.6}Mn_{1.6}O_4$.

FT-IR in the paper showed the phenomenon of Li desorption from different site in order. However, there were little information to explain the orders. It was better to demonstrate it deeply in the energy extent. In the past decades, surface disproportionation mechanism, ion-exchange mechanism, and composite mechanism were proposed as main mechanisms to explain Li^+ intercalation reaction in spinels. In this work of ESI, we would focus only on the ion-exchange mechanism and try to explain the orders in the energy extent. $LiMn_2O_4$ and its all intermediate products were excluded because their Li-desorption mechanism was almost not ion-exchange mechanism, which was confirmed by FT-IR.

The exchange energies (E_{ex}) from H^+ to Li^+ were calculated to confirm the ion exchange ability of different LMO models.

$Li_{1.33}Mn_{1.67}O_4$:

$$(Li_{8a})_6(Li_{16d})_2Mn_{10}O_{24} + 6HCl \rightarrow H_6(Li_{16d})_2Mn_{10}O_{24} + 6LiCl \quad (1)$$

$$(Li_{8a})_6(Li_{16d})_2Mn_{10}O_{24} + 2HCl \rightarrow (Li_{8a})_6H_2Mn_{10}O_{24} + 2LiCl \quad (2)$$

$Li_{1.6}Mn_{1.6}O_4$:

$$(Li_{8a})_4(Li_{16d})_2Mn_6O_{15} + 4HCl \rightarrow H_4(Li_{16d})_2Mn_6O_{15} + 4LiCl \quad (3)$$

$$(Li_{8a})_4(Li_{16d})_2Mn_6O_{15} + 2HCl \rightarrow (Li_{8a})_4H_2Mn_6O_{15} + 2LiCl \quad (4)$$

Using $(Li_{8a})_6(Li_{16d})_2Mn_{10}O_{24}$ as an example, the E_{ex} of Li^+ at different positions of LMO to H^+ can be defined as follows:

$$E_{ex\text{-}Li8a} = [(E_{H6\text{-}LMO} + 6E_{LiCl}) - (E_{LMO} + 6E_{HCl\text{-}H6\text{-}LMO})]/6$$

$$E_{ex\text{-}Li16d} = [(E_{H2\text{-}LMO} + 2E_{LiCl}) - (E_{LMO} + 2E_{HCl\text{-}H2\text{-}LMO})]/2$$

$E_{ex\text{-}Li8a}$ and $E_{ex\text{-}Li16d}$ denoted the E_{ex} from Li^+ in the 8a sites and 16d sites to H^+, respectively. E_{LMO}, $E_{H6\text{-}LMO}$, and $E_{H2\text{-}LMO}$ represented the energies of optimized $(Li_{8a})_6(Li_{16d})_2Mn_{10}O_{24}$, $H_6(Li_{16d})_2Mn_{10}O_{24}$, and $(Li_{8a})_6H_2Mn_{10}O_{24}$, respectively. E_{HCl} was the energies of optimized HCl in the cell with the same cell parameters with that of the optimized $(Li_{8a})_6(Li_{16d})_2Mn_{10}O_{24}$. $E_{HCl\text{-}H6\text{-}LMO}$ and $E_{HCl\text{-}H2\text{-}LMO}$ were the energies of optimized HCl in the cell with the same cell parameters of the optimized $H_6(Li_{16d})_2Mn_{10}O_{24}$ and $(Li_{8a})_6H_2Mn_{10}O_{24}$, respectively. All energy values were obtained by considering dipole correction.

The E_{ex} values in Reactions (1) to (4) were 263.3, 279.5, 103.6, and 108.4 kJ/mol, respectively, which meant that the reaction energy between different site Li^+ and H^+ in

$Li_{1.33}Mn_{1.67}O_4$ or $Li_{1.6}Mn_{1.6}O_4$ made little difference. Thus, energy barrier of reaction between Li^+ of different sites with H^+ should be considered.

Table 1. DFT optimized cell parameters of spinel-type LMOs and average charge in Mn atoms.

Models	a(Å)	b(Å)	c(Å)	α(°)	β(°)	γ(°)	V_0(Å^3)	Mn^a
$(Li_{8a})_8Mn_{16}O_{32}$	8.659	8.659	8.659	90.0	90.0	90.0	649.2	0.96
$(Li_{8a})_6(Li_{16d})_2Mn_{10}O_{24}$	6.077	6.077	14.415	90.0	90.0	120.0	461.0	0.91
$H_6(Li_{16d})_2Mn_{10}O_{24}$	5.777	5.777	15.150	90.0	90.0	120.0	437.9	1.04
$(Li_{8a})_6H_2Mn_{10}O_{24}$	6.033	6.033	14.524	90.0	90.0	120.0	457.7	0.99
$H_8Mn_{10}O_{24}$	6.030	6.030	14.077	90.0	90.0	120.0	443.3	1.14
$(Li_{8a})_4(Li_{16d})_2Mn_6O_{15}$	6.025	5.999	10.277	89.8	106.1	119.4	307.0	0.91
$H_4(Li_{16d})_2Mn_6O_{15}$	6.024	6.133	10.988	92.7	104.3	120.0	324.2	0.89
$(Li_{8a})_4H_2Mn_6O_{15}$	6.033	6.060	9.926	89.1	105.5	119.9	300.2	0.99
$H_6Mn_6O_{15}$	6.039	6.206	10.427	88.2	112.0	119.9	308.0	1.19

[a.] Average charges in Mn

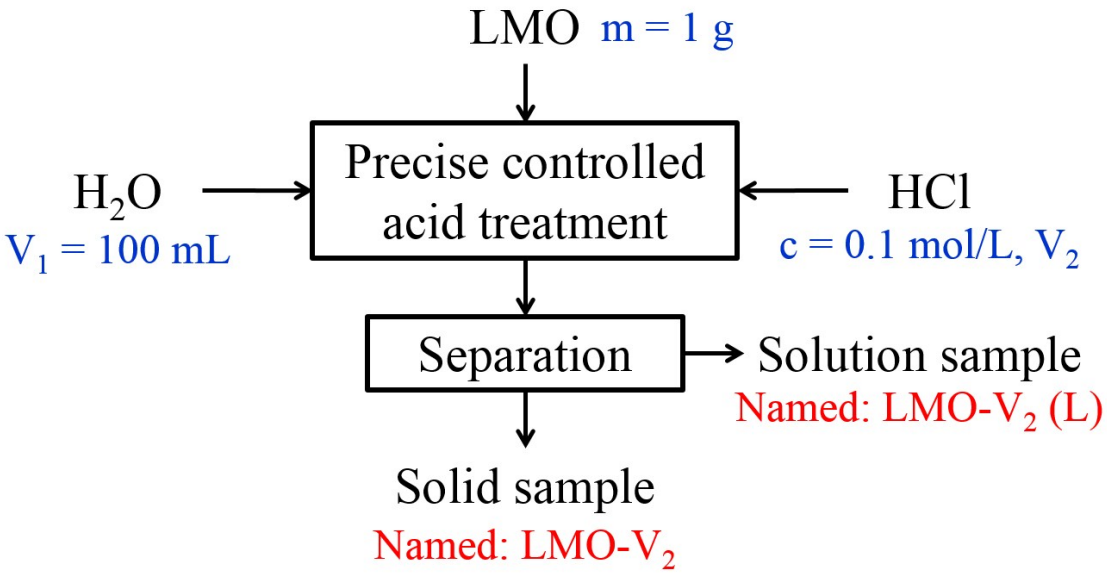

Figure 1. Flow diagram of precise controlled acid treatment.

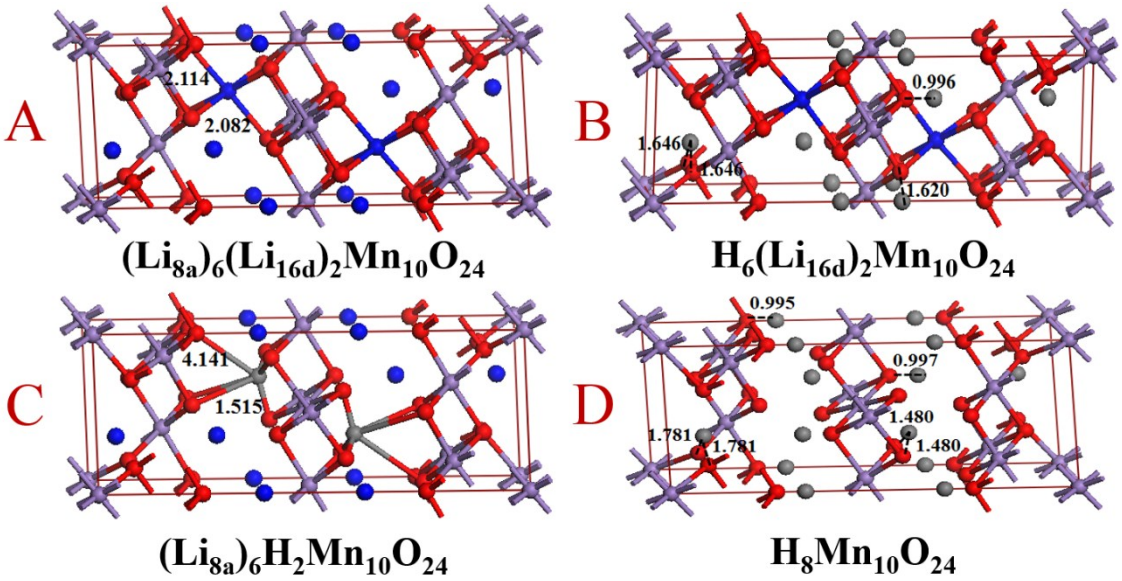

Figure 2(A)-(D). Optimized structure of $(Li_{8a})_6(Li_{16d})_2Mn_{10}O_{24}$ (the same as $Li_{1.33}Mn_{1.67}O_4$) and corresponding protonated compounds (Mn, magenta; O, red; Li, blue; H, grey), which were mentioned in Table 1 of this ESI. Data above were collected by theoretical simulation.

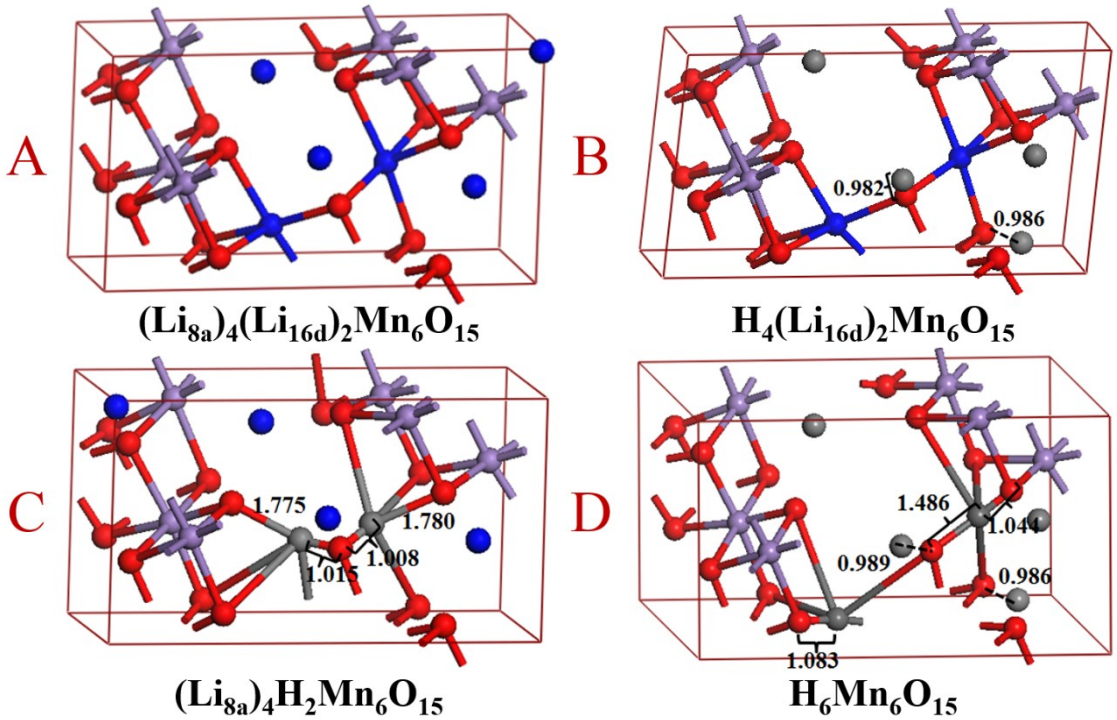

Figure 3(A)-(D). Optimized structure of $(Li_{8a})_4(Li_{16d})_2Mn_6O_{15}$ (the same as $Li_{1.6}Mn_{1.6}O_4$) and corresponding protonated compounds (Mn, magenta; O, red; Li, blue; H, grey), which were mentioned in Table 1 of this ESI. Data above were collected by theoretical simulation.